Materials Transactions, Vol. 44, No. 10 (2003) pp. 2020 to 2024
Special Issue on Nano-Hetero Structures in Advanced Metallic Materials

Origin of Low Coercivity of Fe-(Al, Ga)-(P, C, B, Si, Ge) Bulk Glassy Alloys

Teruo Bitoh[1], Akihiro Makino[1] and Akihisa Inoue[2]

[1]*Department of Machine Intelligence and Systems Science, Faculty of Systems Science of Technology, Akita Prefectural University, Honjo 015-0055, Japan*
[2]*Institute for Materials Research, Tohoku University, Sendai 980-8577, Japan*

The magnetic properties of the glassy Fe-(Al, Ga)-(P, C, B, Si, Ge) alloys have been compared with those of the conventional Fe-based amorphous alloys to clarify the feature of the glassy alloys as a soft magnetic material. The glassy Fe-(Al, Ga)-(P, C, B, Si, Ge) alloys exhibit lower saturation magnetization (J_s) than that of the conventional Fe-(B, Si, C) amorphous alloys with the same Fe content. The glassy alloys also have larger saturation magnetostriction constant (λ_s) than that of the conventional Fe-based amorphous alloys with the same J_s. However, the glassy alloys tend to show relatively low coercivity (H_c) whereas λ_s is large. The theoretical analysis on the basis of domain-wall movement suggests that the low H_c originates from the much higher packing density of the glassy alloys than that of the conventional amorphous alloys, which realizes the low density of the quasi-dislocation dipole-type elastic stress sources or the low pinning force due to the elastic stress. The good combination of high glass-forming ability and good soft magnetic properties (especially low H_c) indicates the possibility of future development as new low loss material.

(Received April 21, 2003; Accepted June 20, 2003)

Keywords: *bulk glassy alloy, iron-based amorphous alloy, soft magnetic property, domain-wall pinning, free volume*

1. Introduction

Since the first success of preparing an amorphous phase in the Au-Si system by rapid solidification in 1960,[1)] a great number of scientific and engineering data for amorphous have been accumulated up to date. As a result, it has been clarified that amorphous alloys have the features of new alloy compositions and new atomic configurations which are different from those for crystalline alloys. These features enable the appearance of various kinds of characteristics such as good mechanical properties, useful physical properties and unique chemical properties[2,3)] which have not been obtained for conventional crystalline alloys.

During the last 15 years, it has been reported that a number of amorphous alloys in Mg-,[4)] lanthanide (Ln)-,[5)] Zr-,[6,7)] Pd-Cu-,[8)] and Ti-[9)] based systems exhibit a wide supercooled liquid region (ΔT_x = crystallization temperature (T_x) − glass transition temperature (T_g)) exceeding 50 K before crystallization. The appearance of the wide supercooled liquid region implies that the alloys have high resistance against crystallization. Consequently, these bulk glassy alloys with large ΔT_x values have been confirmed to have an extremely large glass-forming ability, which enables the production of bulk glassy samples. These bulk glassy alloys have so unique properties that they will be expected to be very useful materials for industrial use. Practically, the Zr-based glassy alloy has been used as a high specific-strength material.

Recently, some kinds of soft magnetic glassy alloys with large ΔT_x combined with good soft magnetic properties have been synthesized in Fe-(Al, Ga)-(P, C, B, Si, Ge)[10–21)] and Fe-(Co, Ni)-(Zr, Nb, Ta, Mo, W)-B systems.[22–24)] The Fe-(Al, Ga)-(P, C, B, Si, Ge) glassy alloys have wide ΔT_x of about 50 K and their maximum thickness to form a single glassy phase is about 220 μm prepared by the single-roller melt-spinning method.[15)] It is interesting that the Fe-(Al, Ga)-(P, C, B, Si, Ge) glassy alloys exhibit good soft magnetic properties, whereas their saturation magnetostriction constant (λ_s) is relatively large.

In this paper, we compare the magnetic properties of the Fe-(Al, Ga)-(P, C, B, Si, Ge) glassy alloys with those of the conventional Fe-based amorphous alloys, and clarify the feature of the glassy alloys as a soft magnetic material. The origin of low coercivity (H_c) of the Fe-(Al, Ga)-(P, C, B, Si, Ge) glassy alloys is discussed.

2. Magnetic Properties of Glassy Fe-(Al, Ga)-(P, C, B, Si, Ge) Alloys Compared with those of Conventional Amorphous Alloys

Table 1 shows the magnetic properties, ΔT_x and maximum sample thickness (t_{max}) for glass formation by single-roller melt-spinning technique of the Fe-(Al, Ga)-(P, C, B, Si, Ge) glassy alloys.[13–16,18)] Here, H_c, λ_s, saturation magnetization (J_s) and ΔT_x are the values for the melt-spun ribbons whose thickness of 20–35 μm. Table 2 shows the magnetic properties of the conventional Fe-(Co, Ni, Al, Ga)-(B, Si, C, P) amorphous alloys.[25–36)] The data of H_c in Tables 1 and 2 show the values after annealing with no-magnetic field. Since H_c of the (Fe, Ni)- or (Fe, Co)-based amorphous alloys strongly depend on induced magnetic anisotropies, only J_s and λ_s are discussed here.

Figure 1 shows J_s as a function of Fe content for the Fe-(Al, Ga)-(P, C, B, Si, Ge) glassy alloys and the conventional amorphous alloys. The J_s values of the glassy alloys are lower than those of the amorphous Fe-(Co, Ni, Ga)-B alloys, and are distributed around the values for the Fe-Al-P-C alloys. All the glassy alloys listed in Table 1 contain P about 10 at%. It has been reported that the replacement of B by P for the conventional Fe-B amorphous alloys considerably decreases J_s.[37)] This implies that to obtain the high J_s comparable to that of the amorphous Fe-(B, Si, C) alloys is difficult for the glassy alloys contain a large amount of P.

It is well-known that λ_s values of Fe-based conventional amorphous alloys are proportional to J_s^2.[31,38)] Figure 2 shows

Table 1 Coercivity (H_c), saturation magnetostriction constant (λ_s), saturation magnetization (J_s), supercooled liquid region (ΔT_x) and maximum sample thickness (t_{max}) for glass formation by single-roller melt-spinning technique of Fe-(Al, Ga)-(P, C, B, Si, Ge) glassy alloys with low H_c.

	No.	Melt-spun ribbons (thickness of 20–35 μm)				t_{max}/μm	Ref.
		H_c/A·m^{-1}	$\lambda_s/10^{-6}$	J_s/T	ΔT_x/K		
$Fe_{80}P_{12}B_4Si_4$	G1	1.1	31	1.34	36	—	13
$Fe_{76}Al_4P_{12}B_4Si_4$	G2	2.6	30	1.24	46	—	13
$Fe_{73}Al_5Ga_2P_{11}C_5B_4$	G3	2.3	24	1.25	48	~135	14
$Fe_{72}Al_5Ga_2P_{11.55}C_{5.25}B_{4.2}$	G4	2.4	21	1.07	50	~140	15, 16
$Fe_{73}Al_{2.86}Ga_{1.14}P_{12.65}C_{5.75}B_{4.6}$	G5	2.7	25	1.30	50	~140	15, 16
$Fe_{77}Al_{2.14}Ga_{0.86}P_{8.4}C_5B_4Si_{2.6}$	G6	2.4	38	1.47	34	~220	15
$Fe_{78}Al_2P_{10}B_6Ge_4$	G7	2.8	41	1.23	30	—	18
$Fe_{75}Al_5P_{10}B_6Ge_4$	G8	2.0	34	1.10	43	—	18
$Fe_{73}Al_5Ga_2P_{10}B_6Ge_4$	G9	2.4	33	1.09	49	—	18

Table 2 Coercivity (H_c), saturation magnetostriction constant (λ_s) and saturation magnetization (J_s) of conventional amorphous alloys prepared by melt-spinning technique (thickness of 20–35 μm).

	H_c/A·m^{-1}	$\lambda_s/10^{-6}$	J_s/T	Ref.
$Fe_{78}B_{22}$	4.7	35	1.55*	25, 26
$Fe_{80}B_{20}$	5.2	35	1.58	25, 26, 27
$Fe_{82}B_{18}$	3.9	33	1.59*	25, 26
$Fe_{84}B_{16}$	4.3	33	1.56*	25, 26
$Fe_{84}B_{16}$	3.6	32	1.53*	25, 26
$Fe_{78}B_{13}Si_9$	2.4	27	1.56	28
$Fe_{81}B_{17}Si_2$	4.0	30	1.61	29
$Fe_{81}B_{13.5}Si_{3.5}C_2$	3.2	30	1.61	28
$Fe_{80}P_{13}C_7$	4.8	30	1.42	27, 30, 31
$Fe_{80}P_{16}C_3B_1$	4.0	29	1.71	32, 33
$Fe_{70}Co_{10}B_{20}$		35	1.65	34, 35
$Fe_{60}Co_{20}B_{20}$		24	1.64	34, 35
$Fe_{50}Co_{30}B_{20}$		24	1.57	34, 35
$Fe_{40}Co_{40}B_{20}$		20	1.5	34, 35
$Fe_{70}Ni_{10}B_{20}$		28	1.55	27, 35
$Fe_{60}Ni_{20}B_{20}$		24	1.39	27, 35
$Fe_{50}Ni_{30}B_{20}$		17	1.23	27, 35
$Fe_{40}Ni_{40}B_{20}$		14	1.04	27, 35
$Fe_{76}Al_4P_{13}C_7$		24	1.32**	31
$Fe_{72}Al_8P_{13}C_7$		20	1.22**	31
$Fe_{79}Ga_1B_{20}$			1.57*	36
$Fe_{78}Ga_2B_{20}$			1.56*	36
$Fe_{77}Ga_3B_{20}$			1.53*	36

* Relative value for $Fe_{80}B_{20}$.
** Relative value for $Fe_{80}P_{13}C_7$.

λ_s for the glassy alloys and the conventional amorphous alloys as a function of J_s^2. The saturation magnetostriction constants of both the systems are nearly proportional to J_s^2. The Fe-(Al, Ga)-(P, C, B, Si, Ge) glassy alloys exhibit higher λ_s compared with that of the conventional amorphous alloys with the same J_s. Especially, the Si or Ge contain alloys (G1, G2, G6-G9) exhibit rather large λ_s. It has been reported that the replacement of B by Si for the conventional Fe-B amorphous alloys increases λ_s.[39,40] As well as the conventional amorphous alloys, it is considered that the addition of Si or Ge, which belongs to the same IVb group as Si, to the glassy alloys increases λ_s.

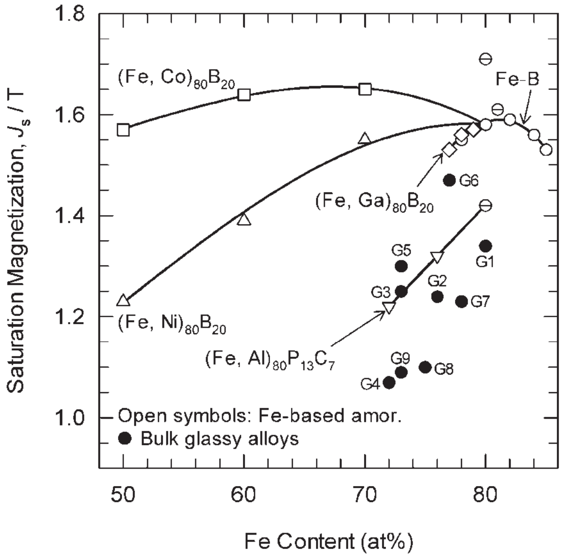

Fig. 1 Saturation magnetization (J_s) as a function of Fe content for Fe-based glassy alloys and conventional amorphous alloys.

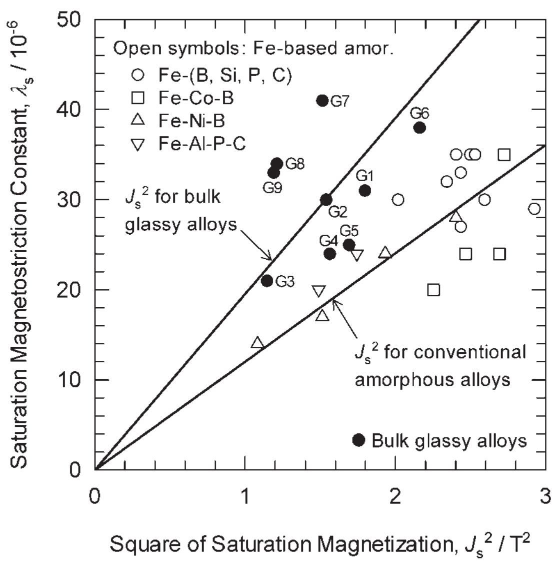

Fig. 2 Saturation magnetostriction constant (λ_s) as a function of square of saturation magnetization (J_s) for Fe-based glassy alloys and conventional amorphous alloys.

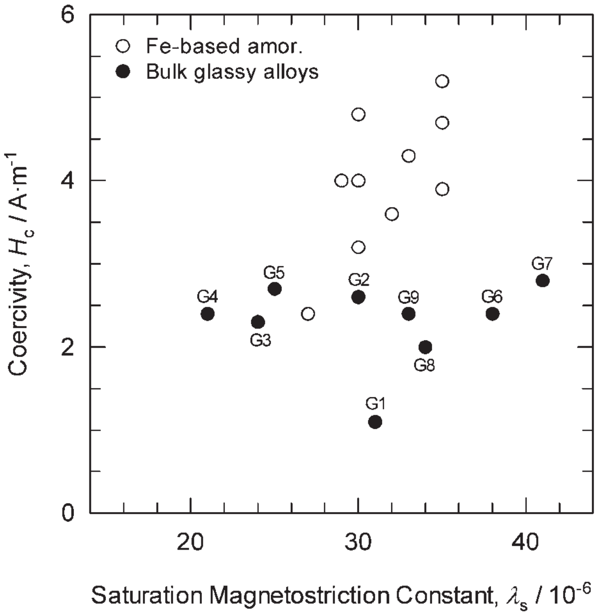

Fig. 3 Relationship between coercivity (H_c) after annealing and saturation magnetostriction constant (λ_s) for Fe-based glassy alloys and conventional amorphous alloys.

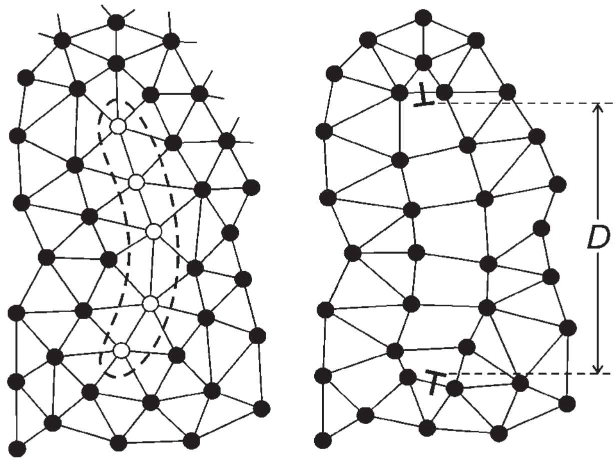

Fig. 4 Schematic two-dimensional model for formation of quasi-dislocation dipoles in amorphous alloys by agglomeration of vacancy-type point defects in planar regions.[43,47,53] The quasi-dislocation dipole is characterized by dipole width (D), dipole length (L_3) perpendicular to the drawing plane and an effective Burgers vector ($\boldsymbol{b}$).

Figure 3 shows the relationship between H_c and λ_s for the melt-spun Fe-(Al, Ga)-(P, C, B, Si, Ge) glassy alloys and the conventional amorphous alloys. The typical Fe-based amorphous alloys such as Fe-B, Fe-Si-B and Fe-P-C exhibit relatively large λ_s (about 30×10^{-6}) and H_c ($\geq$2.4 A/m). The coercivity of the alloys decreases with decreasing λ_s. On the other hand, λ_s of the Fe-(Al, Ga)-(P, C, B, Si, Ge) glassy alloys is about 20–40 $\times 10^{-6}$. However, the glassy alloys tend to show low H_c whereas λ_s is large. Especially, the $Fe_{78}Al_2P_{10}B_6Ge_4$ alloy (G7) exhibits large λ_s of 41×10^{-6}, however, its H_c is only 2.8 A/m.

3. Discussion

The coercivity is controlled by the process of magnetization reversal and thus depends on magnetic nucleation, rotation of magnetic moments and domain-wall motion. The rotation of magnetization and domain-wall motion are associated with the anisotropy, strain, exchange interaction, demagnetizing effects and the presence of structural and surface inhomogeneities. If the magnetization reversal takes place by domain-wall motion, this process involves local magnetic nucleation and domain expansion controlled by the presence of defects, local magnetic inhomogeneities, surface roughness or intrinsic magnetic fluctuations caused by structural disorder.[41–45] In crystalline materials H_c is determined by dislocations and grain boundaries. In amorphous materials both kind of defects in the conventional picture do not exist. Nevertheless, the observed H_c has values of the order of magnitude 0.5–10 A/m which are considerably larger then the expected ones for the intrinsic inhomogeneities ($\leq 3 \times 10^{-5}$ A/m) or short-range order ($\leq 1 \times 10^{-4}$ A/m).[44] The typical value for the contribution of the surface roughness to H_c has been estimated to be 0.5 A/m for Fe-based amorphous alloys and thus represents one of the limiting factors for H_c of the amorphous alloys.[44,45] It is therefore suggested that in amorphous alloys exist inhomogeneities acting as strong pinning centers for domain walls. These pinning centers were found to correspond to stress sources.

Stress sources are supposed to have their origin in the partial instability of the free volume below the melting point. The free volume may exist in dispersed form as the melt of in the form of agglomerates. However, three-dimensional clusters of vacancy-type are supposed to be unstable.[46] By a relaxation of the atomic network the vacancy clusters may collapse thus generating planar defects which act as stress source.[43,47,48] The dispersed free volume is similar to partial point defects with stress fields varying as r^{-3} (r is the distance from the stress center) whereas planar defects are equivalent to dislocation dipoles (quasi-dislocation dipoles) with stress fields varying as r^{-2}.[43] Figure 4 shows a model for formation of the quasi-dislocation dipoles in amorphous alloys by agglomeration of vacancy-type point defects.[43,47,49] The quasi-dislocation dipoles generate short-range (but longer than domain-wall thickness) stress fields and act as pinning centers for domain walls.[43,47,48] The type of stress sources existing in amorphous alloys has been investigated by means of the low of approach to ferromagnetic saturation.[47,49] Form the high-field susceptibility it was derived that the quasi-dislocation dipoles are the main sources of elastic stress.[43,47,48]

The quasi-dislocation dipoles are characterized by the dipole width (D), the dipole length (L_3) and an effective Burgers vector ($\boldsymbol{b}$) with components b_1 and b_2 as shown in Fig. 5,[44,45] where the coordination axis x_1 is orientated parallel and the axis x_3 is perpendicular to the easy axis, and the x_2-axis was chosen to be parallel to the domain-wall normal. Kronmüller and his co-workers calculated H_c of a random distribution of the quasi-dislocation dipoles of densities ρ_d based on the statistical potential theory.[43–45,50–53] In the special case of the quasi-dislocation dipoles with $\varepsilon = \pi/2$, $b_3 = 0$ and $b_1 = b$, they obtain[43–45]

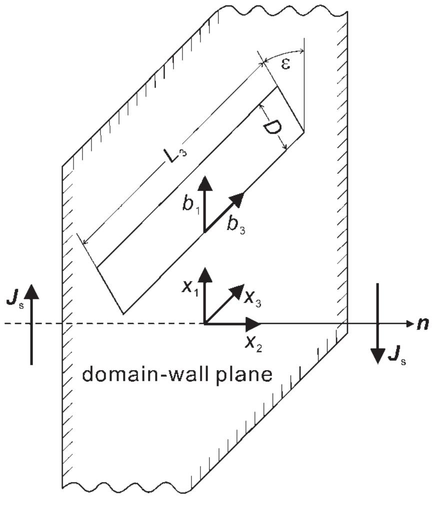

Fig. 5 Geometry of a quasi-dislocation dipole interacting with a domain wall.[44,45)]

$$H_c = \frac{12G\Delta V}{\sqrt{30F\delta}}\sqrt{\pi\rho_d \ln\left(\frac{\pi L_2}{2\delta}\right)}\frac{\lambda_s}{J_s}, \qquad (1)$$

where G is the shear modulus,

$$\Delta V = DL_3 b \qquad (2)$$

corresponds to the volume contraction due to the quasi-dislocation dipoles, F is the domain-wall area, L_2 is the domain width, respectively. The domain-wall thickness,

$$\delta = \pi\sqrt{\frac{A}{K}}, \qquad (3)$$

is determined by the micromagnetic exchange stiffness constant (A) and the anisotropy constant (K). The factor of $\ln\{\pi L_2/(2\delta)\}$ in eq. (1) takes into account the statistical fluctuations due to the $\pi L_2/(2\delta)$ independent positions of the domain wall within the domain width. The parameters were derived from the high-field susceptibility of the $Fe_{40}Ni_{40}B_{20}$ conventional amorphous alloy as follows:[48,49)] $D \approx 10$ nm, $L_3 \approx 50$ nm, $b \approx 0.2$ nm, $\rho_d \approx 2 \times 10^{23}$ m^{-3}, $F \approx 6 \times 10^{-9}$ m^2, $\delta \approx 300$ nm and $L_2 \approx 100$ µm. Numerical calculations based on eq. (1) predict values for H_c in magnetostrictive alloys of the right order of magnitude, while measurements of the temperature dependence of $H_c J_s/\lambda_s$, which should correspond to $\delta^{-1/2} \propto K^{1/4}$, in a number of Fe-based amorphous alloys have provided convincing proof for the existence and role of the quasi-dislocation dipoles.[43–45)] It should be noted that eq. (1) gives the similar result to the well-known Kersten's relation with long-range stress fields,[54)] $H_c = \pi\lambda_s\sigma_0\delta/(2J_s l)$, where σ_0 and l are the amplitude and the wave-length of the internal stress. However, it gives $H_c J_s/\lambda_s \propto \delta \propto K^{-1/2}$, which is different from the observed relation ($H_c J_s/\lambda_s \propto K^{1/4}$) in Fe-based amorphous alloys.

If G, F, δ and L_2 of the glassy alloys are the same as those of the conventional amorphous alloys as shown in Tables 1 and 2, respectively, H_c can be written as

$$H_c \propto \Delta V\sqrt{\rho_d}\frac{\lambda_s}{J_s}. \qquad (4)$$

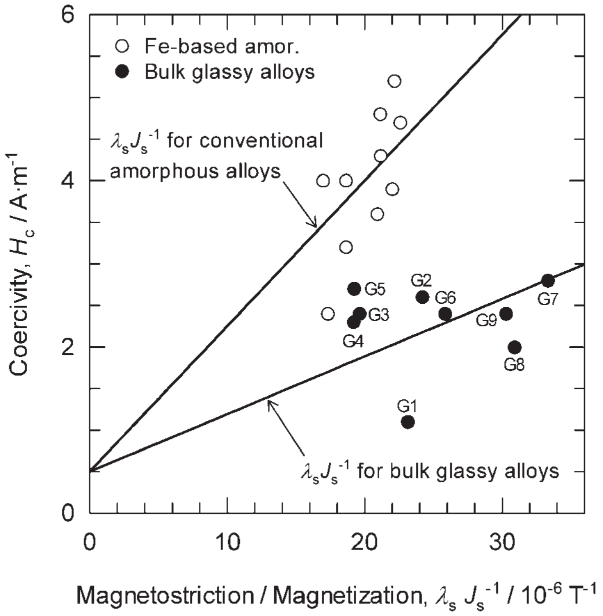

Fig. 6 Coercivity (H_c) after annealing as a function of saturation magnetostriction constant/saturation magnetization (λ_s/J_s) for melt-spun Fe-based glassy alloys and conventional amorphous alloys. Contribution of surface irregularities to H_c is assumed to be 0.5 A/m.[44,45)]

Figure 6 shows H_c as a function of λ_s/J_s for the glassy Fe-(Al, Ga)-(P, C, B, Si, Ge) alloys and conventional amorphous alloys. Here, the contribution of the surface irregularities to H_c is assumed to be 0.5 A/m.[44,45)] It should be noted that the glassy Fe-(Al, Ga)-(P, C, B, Si, Ge) alloys exhibit lower H_c than the conventional amorphous alloys with the same λ_s/J_s. The gradient of the H_c vs. λ_s/J_s plot for the glassy alloys is smaller than that for the conventional amorphous alloys. This result indicates that $\Delta V\rho_d^{1/2}$ of the glassy alloys is about 0.4 as large as that of the conventional amorphous alloys. This result suggests that ρ_d of the glassy alloys is about 0.16 as large as that of the conventional amorphous alloys or ΔV of the glassy alloys is about 0.4 as large as that of the conventional amorphous alloys. Here, the decrease of ΔV means the decrease in the pinning force due to the elastic stress.[43–45)] It should be noted that ΔV and ρ_d strongly depends on the quenched-in free volume descried above. It has been reported that the difference in the mass densities ($\Delta\rho_m^{ga}$) between the as-cast amorphous and fully crystallized states of the bulk glassy alloys is in the range of 0.30–0.54%,[55)] which is much smaller than that of the conventional amorphous alloys ($\Delta\rho_m^{ca} \propto 2$–3%).[2,56)] It should be noted that $\Delta\rho_m^{ga}/\Delta\rho_m^{ca}$ (≈0.1–0.3) is consistent with the above results.

It is possible that H_c of Fe-based amorphous alloys is decreased by various techniques. For example, low H_c values of 1–1.5 A/m have been obtained for amorphous Fe-Cr-Si-B alloys annealed in no-magnetic field followed by water quenching,[57)] and for amorphous Fe-B-C(-Si) alloys annealed and slowly cooled in a static magnetic field.[58)] It should be noted that these techniques may be effective for the Fe-based glassy alloys, *i.e.*, further low H_c will be obtained for the glassy alloys. It can be said that the Fe-based glassy alloys have the high possibility as a new low loss material.

4. Conclusions

The relationship among J_s, λ_s and H_c of the glassy Fe-(Al, Ga)-(P, C, B, Si, Ge) alloys is discussed. The glassy alloys tend to show relatively low H_c whereas λ_s is large. The theoretical analysis on the basis of domain-wall movement suggests that the main part of H_c should be proportional to $\Delta V \rho_d{}^{1/2} \lambda_s / J_s$. These results suggest that the low H_c originates from the much higher packing density of the glassy alloys than that of the conventional amorphous alloys, which realizes the low density of the quasi-dislocation dipole-type elastic stress sources or the low pinning force due to the elastic stress. The good combination of high glass-forming ability and good soft magnetic properties (especially low H_c) indicates the possibility of future development as a new bulk glassy soft magnetic material.

Acknowledgements

This work was supported by the New Energy and Industrial Technology Development Organization (NEDO) through the R&D Institute of Metals and Composites for Future Industries (RIMCOF).

REFERENCES

1) W. Klement, R. H. Willens and P. Duwez: Nature **187** (1960) 869–870.
2) H. S. Chen: Rep. Prog. Phys. **43** (1980) 353–432.
3) *Materials Science of Amorphous Metals*, ed. by T. Masumoto (Ohm, Tokyo, 1982).
4) A. Inoue, K. Ohtera, K. Kita and T. Masumoto: Jpn. J. Appl. Phys. **27** (1988) L2248–L2251.
5) A. Inoue, T. Zhang and T. Masumoto: Mater. Trans., JIM **30** (1989) 965–972.
6) A. Inoue, T. Zhang and T. Masumoto: Mater. Trans., JIM **31** (1990) 177–183.
7) A. Peker and W. L. Johnson: Appl. Phys. Lett. **63** (1993) 2342–2344.
8) A. Inoue, N. Nishiyama and T. Masuda: Mater. Trans., JIM **37** (1996) 181–184.
9) K. Amiya, N. Nishiyama, A. Inoue and T. Masumoto: Mater. Sci. Eng. A **179/180** (1994) 692–696.
10) A. Inoue and J. S. Gook: Mater. Trans., JIM **36** (1995) 1180–1183.
11) A. Inoue, Y. Shinohara and J. S. Gook: Mater. Trans., JIM **36** (1995) 1427–1433.
12) A. Inoue, A. Takeuchi, T. Zhang, A. Murakami and A. Makino: IEEE Trans. Magn. **32** (1996) 4866–4871.
13) A. Inoue and R. E. Park: Mater. Trans., JIM **37** (1996) 1715–1721.
14) T. Mizushima, A. Makino and A. Inoue: Mater. Sci. Eng. A **226–228** (1997) 721–725.
15) T. Mizushima, S. Yoshida, A. Makino and A. Inoue: J. Magn. Soc. Jpn. **22** (1998) 1085–1089.
16) T. Mizushima, A. Makino, S. Yoshida and A. Inoue: Mater. Res. Soc. Symp. Proc., ed. by W. L. Johnson, A. Inoue and C. T. Liu (Materials Research Society, Warrendale, 1999) vol. 554, pp. 155–160.
17) T. Mizushima, K. Ikarashi, S. Yoshida, A. Makino and A. Inoue: Mater. Trans., JIM **40** (1999) 1019–1022.
18) R. E. Park and A. Inoue: Mater. Trans., JIM **40** (1999) 1444–1449.
19) B. Shen, H. Koshiba, T. Mizushima and A. Inoue: Mater. Trans., JIM **41** (2000) 873–876.
20) A. Makino, A. Inoue and T. Mizushima: Mater. Trans., JIM **41** (2000) 1471–1477.
21) B. Shen, H. Kimura, A. Inoue and T. Mizushima: Mater. Trans. **42** (2001) 660–663.
22) A. Inoue, T. Zhang, T. Itoi and A. Takeuchi: Mater. Trans., JIM **38** (1997) 359–362.
23) A. Inoue, H. Koshiba, T. Zhang and A. Makino: Mater. Trans., JIM **38** (1997) 577–582.
24) A. Inoue, T. Zhang and A. Takeuchi: Appl. Phys. Lett. **71** (1997) 464–466.
25) R. C. O'Handley, M. C. Narasimhan and M. O. Sullivan: J. Appl. Phys. **50** (1979) 1633–1635.
26) F. E. Luborsky, H. H. Liebermann, J. J. Becker and J. L. Walter: Proc. 3rd Int. Conf. Rapidly Quenched Metals (The Metals Society, London, 1978), vol. 2, pp. 188–196.
27) J. J. Becker, F. E. Luborsky and J. L. Walter: IEEE Trans. Magn. **MAG-13** (1977) 988–991.
28) C. H. Smith: IEEE Trans. Magn. **MAG-18** (1982) 1376–1381.
29) K. Mohri and S. Takeuchi: IEEE Trans. Magn. **MAG-17** (1981) 3379–3381.
30) H. Fujimori, T. Masumoto, Y. Obi and M. Kikuchi: Jpn. J. Appl. Phys. **13** (1974) 1889–1890.
31) S. Ito, K. Aso, Y. Makino and S. Uedaira: Appl. Phys. Lett. **37** (1980) 665–666.
32) R. C. O'Handley: AIP Conf. Proc. **29** (1976) 206–208.
33) P. J. Flanders, C. D. Graham Jr. and T. Egami: IEEE Trans. Magn. **MAG-11** (1975) 1323–1325.
34) R. C. O'Handley, R. Hasegawa, R. Ray and C.-P. Chou: Appl. Phys. Lett. **29** (1976) 330–332.
35) R. C. O'Handley: Phys. Rev. B **18** (1978) 930–938.
36) F. E. Luborsky, J. L. Walter and H. H. Liebermann: IEEE Trans. Magn. **MAG-17** (1981) 3467–3470.
37) C. D. Graham and T. Egami: IEEE Trans. Magn. **MAG-15** (1979) 1398–1403.
38) R. C. O'Handley: Solid State Commun. **21** (1977) 1119–1122.
39) F. E. Luborsky, P. J. Flanders, H. H. Liebermann and J. L. Walter: IEEE Trans. Magn. **MAG-15** (1979) 1961–1962.
40) T. Jagielinski: IEEE Trans. Magn. **MAG-17** (1981) 2825–2830.
41) P. Dekker: IEEE Trans. Magn. **MAG-12** (1976) 311–327.
42) E. M. Gyorgy: *Metallic Glasses*, ed. by J. J. Gilman and H. J. Leamy (American Society for Metals, Metals Park, 1978) pp. 275–303.
43) H. Kronmüller: J. Appl. Phys. **52** (1981) 1859–1864.
44) H. Kronmüller: J. Magn. Magn. Mater. **24** (1981) 159–167.
45) H. Kronmüller and B. Gröger: J. de Phys. **42** (1981) 1285–1292.
46) C. H. Bennett, P. Chaudhari, V. Moruzzi and P. Steinhardt: Phil. Mag. A **40** (1979) 485–495.
47) H. Kronmüller, M. Fähnle, M. Domann, H. Grimm, R. Grimm and B. Gröger: J. Magn. Magn. Mater. **13** (1979) 53–70.
48) H. Kronmüller: J. de Phys. **41**, C8 (1980) 618–625.
49) H. Kronmüller: IEEE Trans. Magn. **MAG-15** (1979) 1218–1225.
50) K.-H. Pfeffer: Phys. Status Solidi **21** (1967) 857–872.
51) H. Kronmüller: Z. Angew. Phys. **30** (1970) 9–13.
52) H. Kronmüller: AIP Conf. Proc. **10** (1973) 1006–1025.
53) B. Gröger and H. Kronmüller: Appl. Phys. **24** (1981) 287–297.
54) S. Chikazumi: *Physics of Ferromagnetism* (Shokabo, Tokyo, 1984) vol. II, pp. 225–276.
55) A. Inoue, T. Negishi, H. Kimura, T. Zhang and A. R. Yavari: Mater. Trans., JIM **39** (1998) 318–321.
56) T. Masumoto, H. Kimura, A. Inoue and Y. Waseda: Mater. Sci. Eng. **23** (1976) 141–144.
57) K. Inomata, M. Hasegawa and S. Shimanukim: IEEE Trans. Magn. **MAG-17** (1981) 3076–3078.
58) M. Mitera, T. Masumoto and N. S. Kazama: J. Appl. Phys. **50** (1979) 7609–7611.